Journal of Composite Materials
http://jcm.sagepub.com/

Investigating Silica Nanoparticle Effect on Dynamic and Quasi-static Compressive Strengths of Glass Fiber/Epoxy Nanocomposites

Jia-Lin Tsai and Yi-Lieh Cheng

Journal of Composite Materials 2009 43: 3143 originally published online 9 September 2009
DOI: 10.1177/0021998309345317

The online version of this article can be found at:
http://jcm.sagepub.com/content/43/25/3143

Published by:
SAGE
http://www.sagepublications.com

On behalf of:

American Society for Composites

Additional services and information for *Journal of Composite Materials* can be found at:

Email Alerts: http://jcm.sagepub.com/cgi/alerts

Subscriptions: http://jcm.sagepub.com/subscriptions

Reprints: http://www.sagepub.com/journalsReprints.nav

Permissions: http://www.sagepub.com/journalsPermissions.nav

Citations: http://jcm.sagepub.com/content/43/25/3143.refs.html

>> Version of Record - Nov 25, 2009

OnlineFirst Version of Record - Sep 9, 2009

Downloaded from jcm.sagepub.com by NATIONAL CHIAO TUNG UNIV LIB on April 24, 2014

What is This?

Investigating Silica Nanoparticle Effect on Dynamic and Quasi-static Compressive Strengths of Glass Fiber/Epoxy Nanocomposites

JIA-LIN TSAI* AND YI-LIEH CHENG
Department of Mechanical Engineering, National Chiao Tung University
Hsinchu, Taiwan 300

ABSTRACT: The research is aimed to investigate the compressive strengths of glass/epoxy nanocomposites, containing various loadings of spherical silica nanoparticles. Through a sol–gel technique, the silica particles with a diameter of 25 nm were exfoliated uniformly into the epoxy resin. Subsequently, by inserting the silica–epoxy mixture into the unidirectional glass fiber through a vacuum hand lay-up process, the glass fiber/epoxy composite laminates with 10, 20, and 30 wt% of silica nanoparticles were fabricated. Quasi-static and dynamic compression tests were conducted on the brick composite specimens with fiber orientations of 0°, 5°, 10°, 15°, and 90° using a hydraulic MTS machine and a split Hopkinson pressure bar, respectively. Observations on the failure specimens indicated that for fiber orientations less than 15°, the fiber microbuckling is the dominant failure mechanism. On the other hand, for the 90° samples, the out-of-plane shear failure is the main failure mechanism. In addition, it was denoted that as the silica contents increase, the compressive strengths of the glass/epoxy composites are improved accordingly. The enhancing mechanism in the compressive strengths can be properly explicated using the microbuckling model.

KEY WORDS: silica nanocomposites, compressive strength, Split Hopkinson Pressure Bar.

INTRODUCTION

WITH EXTENSIVE APPLICATIONS of composites, the demand for the materials possessing the characteristics of high stiffness and strength is increasing. However, because the compressive strengths of fiber composites are lower when compared to its tensile strength, the compressive failures have been of great concern to the composite community.

*Author to whom correspondence should be addressed. E-mail: jialin@mail.nctu.edu.tw
Figures 1, 3, 4 and 7–9 appear in color online: http://jcm.sagepub.com

0021-9983/09/25 3143–13 $10.00/0 DOI: 10.1177/0021998309345317
© The Author(s), 2009. Reprints and permissions:
http://www.sagepub.co.uk/journalsPermissions.nav

Downloaded from jcm.sagepub.com at NATIONAL CHIAO TUNG UNIV LIB on April 24, 2014

In past decades, the compressive strengths of unidirectional composites were effectively predicted by using either the microbuckling model [1,2] or the kink-band model [3,4]. It was suggested that the compressive failure of a fiber composite in the form of fiber microbuckling is governed by the matrix stiffness property. Thus, it is reasonable to expect a pronounced improvement of compressive strength if the matrix properties can be modified appropriately. Based on the aforementioned concept, Subramaniyan and Sun [5] demonstrated that the longitudinal compressive strength of glass fiber reinforced composites could be improved properly by using nanoclay-modified matrix.

Spherical particles have been used as reinforcement in polymeric materials for many years. In general, these particle sizes were in micron ranges. However, with the advance of nanotechnology as well as the processing techniques, various types of particles with nanoscale have recently been developed and then utilized in conventional polymeric materials to form the nanocomposites. Rosso et al. [6] employed the well-dispersed silica nanoparticles as reinforcement in composites, indicating that the addition of 5 vol% silica nanoparticles could improve the stiffness and fracture energy to 20% and 140%, respectively. The similar escalating behaviors were also observed by Johnsen et al. [7]. Considering the superior mechanical properties of silica nanoparticles, Zheng and Ning [8] adopted the silica nanocomposites as matrix material in conjunction with the glass fiber to form hybrid glass/silica/epoxy nanocomposites. They found that the bending properties as well as the tensile properties of the fiber composites were enhanced by the addition of silica nanoparticles. The enhancement could be attributed to the promoted bonding forces between the glass fiber and matrix modified by the silica nanoparticles. In light of the forgoing investigation, it was concluded that the silica nanoparticles can significantly enhance the mechanical behaviors of polymeric materials as well as the tensile and bending properties of glass fiber composites. Recently, Uddin and Sun [9] indicated that inclusion of silica nanoparticles can significantly increase the longitudinal compressive strength of fiber composites and moderately improve the longitudinal and transverse tensile strengths. Moreover, the improvement in compressive strength is much pronounced in high fiber volume fraction nanocomposites than the low fiber volume fraction nanocomposites.

In this study, systematic experimental investigations were carried out to understand the effect of silica nanoparticles on quasi-static and dynamic compressive behaviors of glass fiber/epoxy composites. Off-axis brick specimens with fiber orientations of 0°, 5°, 10°, 15°, and 90° were tested to failure using a hydraulic MTS machine and a Split Hopkinson Pressure Bar (SHPB), respectively, from which the quasi-static and dynamic compressive strengths were determined accordingly. All failure samples were examined using scanning electron microscopy (SEM) to determine the corresponding failure mechanism.

Sample Preparations

In order to investigate the silica nanoparticle effect on the compressive strength, the glass fiber/epoxy brick specimens with various loadings of silica particles were prepared. The epoxy resin used in this study is Nanopox@ F400, which was supplied from Hanse Chemie, Germany. Basically, it is a diglycidyl ether of bisphenol A (DGEBA) resin, containing 40 wt% silica nanoparticles. Through sol–gel processing, the synthesized silica particles were dispersed uniformly in DGEBA resin [10]. The curing agent used is Jeffamine D-230 (polyoxypropylenedi amine with a molecular weight of 230) provided by the Huntsman Corporation. To have a desired amount of silica contents in the specimens, the Nanopox@ F400 resin was diluted at the beginning by adding a desired amount of

Downloaded from jcm.sagepub.com at NATIONAL CHIAO TUNG UNIV LIB on April 24, 2014

DGEBA resin. The mixture was then sonicated using a sonicator with a cooling system around the sample container until the particles were displaced uniformly in the epoxy resin. The epoxy–silica mixture was degassed at room temperature in a vacuum oven for 10 min and then mixed with the curing agent. The mechanical stirrer was utilized to blend the final mixture at room temperature for 10 min. Afterward, vacuum-assisted hand lay-up procedures were adopted for preparing the glass fiber/silica/epoxy nanocomposites. The mixture of silica/epoxy and the D-230 curing agent was poured on one dry unidirectional glass fiber layer (provided by Vectorply®, E-LR0908-14 unidirectional E-glass fiber). The compound was impregnated into the dry fiber using a hand roller until the fiber bundles were permeated completely by the resin. Then, another ply of dry fiber was stacked on it. The repeating process continued until the 22 layers of glass fibers were fabricated. The fiber stack was sandwiched between two steel plates with porous Teflon fabric on the surfaces, and it was then sealed within a vacuum bag. The whole laminates were cured in a hot press with a suggested temperature profile under vacuum conditions. It is noted that the vacuum is an essential process for forming nanocomposites because it can facilitate the removal of the tiny bubbles trapped in the nanocomposites. In this study, the laminates consisting of 0, 10, 20, and 30 wt% silica nanoparticles were prepared. Off-axis brick specimens with fiber orientations of 0°, 5°, 10°, 15°, and 90° with dimensions of $8 \times 6 \times 6\,\text{mm}^3$ as shown in Figure 1 were cut from the laminates using a diamond wheel. The fiber volume fraction for all the off-axis specimens is around 45%.

In order to evaluate the quality of dispersion of the silica nanoparticles in the epoxy matrix, the epoxy samples were examined using a transmission electron microscope (TEM). Samples with around 70 nm thickness for TEM analysis were prepared using a microtome at the cryogenic condition. TEM observations of epoxy/silica nanocomposites were carried out by a JEOL 200CX with an acceleration voltage of 120 kV. The micrographics of the nanocomposites with 20 wt% silica nanoparticles at 50,000 and 100,000 magnifications were illustrated, respectively, in Figure 2. It was shown that the particles were well dispersed and homogeneously distributed in the nanocomposites. In addition, most of the nanoparticles were in spherical shape, and the average diameter was around 25 nm.

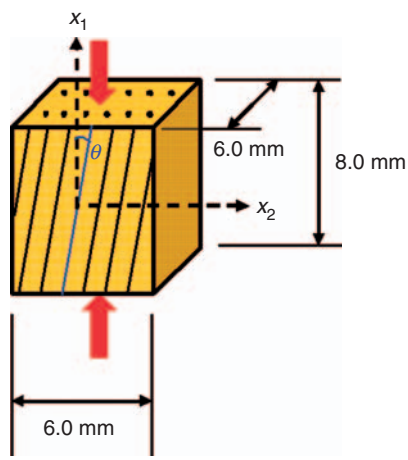

Figure 1. *Dimensions of brick specimens.*

Downloaded from jcm.sagepub.com at NATIONAL CHIAO TUNG UNIV LIB on April 24, 2014

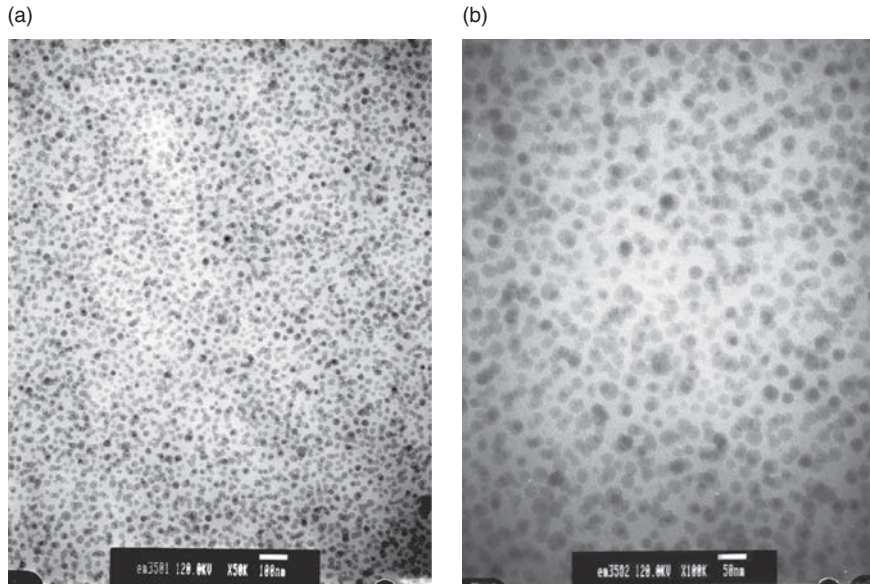

Figure 2. *TEM micrographs of epoxy/silica nanocomposites (20 wt% silica nanoparticles): (a) 50,000, (b) 100,000.*

Therefore, based on the TEM observations, it was suggested that the present samples were regarded as the nanocomposites with fully dispersed spherical nanoparticles.

Experimental Procedure

In order to understand the silica particle influence on the compressive strengths, the fiber composites with various silica loadings were tested to failure under compressive loadings. Both quasi-static and dynamic compression tests were performed on the samples using a conventional hydraulic MTS machine and a SHPB, respectively.

Quasi-Static Compression Tests

Off-axis brick specimens with fiber orientations of 0°, 5°, 10°, 15°, and 90° (against the long direction) were employed for the measurement of compressive strengths. The brick specimens were lapped on a lapping machine with 3 μm abrasive slurry to ensure smooth and flat loading surfaces. In addition, a lubricant was applied to the end surfaces of the specimen to reduce contact friction. The compressive forces were applied to the samples through the end loading fixture attached by a pair of tungsten carbide disks as shown in Figure 3. A self-adjusting device, as shown in Figure 3, was used to eliminate potential bending moments and also to ensure that the specimen was in full contact with the loading surfaces. All tests were conducted at a hydraulic MTS machine with a strain rate of $0.0001\,s^{-1}$. The applied load and displacement for each test were recorded using LabVIEW software with a PC computer. The maximum value in the load–displacement curve was regarded as the failure stress of the sample in the quasi-static tests.

Downloaded from jcm.sagepub.com at NATIONAL CHIAO TUNG UNIV LIB on April 24, 2014

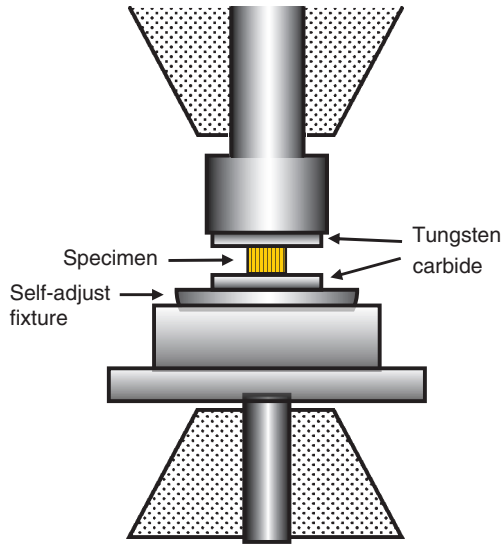

Figure 3. *Schematic of quasi-static compression tests.*

Dynamic Compression Tests

High strain–rate experiments were conducted using a SHPB, which is a simple and effective device for dynamic tests. The SHPB setup used in this study was made of hardened steel bars, which were 13.3 mm in diameter, as shown in Figure 4. The striker bar had a length of about 90 mm, and the incident bar and the transmission bar were 91 and 56 cm long, respectively. The off-axis brick specimens employed in the SHPB tests were the same as those used for the quasi-static tests. During the tests, the brick specimen was sandwiched between the incident bar and the transmission bar. It is noted that shear-extension coupling takes place in off-axis specimens under axial loading. This behavior combined with bar-specimen interfacial friction could give rise to inhomogeneous deformation in the specimen, resulting in deviations from the conventional Hopkinson bar assumption. In order to reduce the interfacial friction, all test specimens were lapped and lubricated as suggested by Ninan et al. [11]. In addition, a pulse shaper technique was used to produce a gently rising loading pulse that would help in extracting reliable stress–strain curves from SHPB tests. This pulse shaping can be achieved using a piece of soft material inserted between the striker bar and the incident bar. A copper tab that was 1.7 mm thick was used as the pulse shaper in the present study.

A pair of diametrically opposite gages (gage A), as shown in Figure 4, was mounted on the incident bar to measure both the incident and reflected signals. On the other hand, in the transmission bar, strain gages (gage B) were mounted at about 160 mm from the bar/specimen interface to measure the transmitted pulse. The strain gages on the bars were connected to Wheatstone circuits and then amplified using a conditioning amplifier. Finally, the signals were recorded by the digital oscilloscope with a sampling rate of 10 MHz. Figure 5 shows the typical strain gage signals measured from the incident and transmission bars, respectively. Based on 1D wave propagation theory [12], the contact stress P_1, between the incident bar and the specimen, and P_2, the contact stress between the

Downloaded from jcm.sagepub.com at NATIONAL CHIAO TUNG UNIV LIB on April 24, 2014

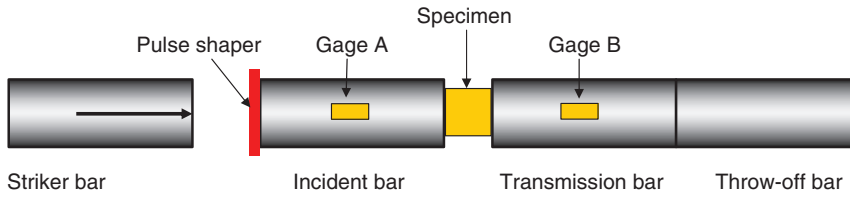

Figure 4. *Schematic of SHPB fixture.*

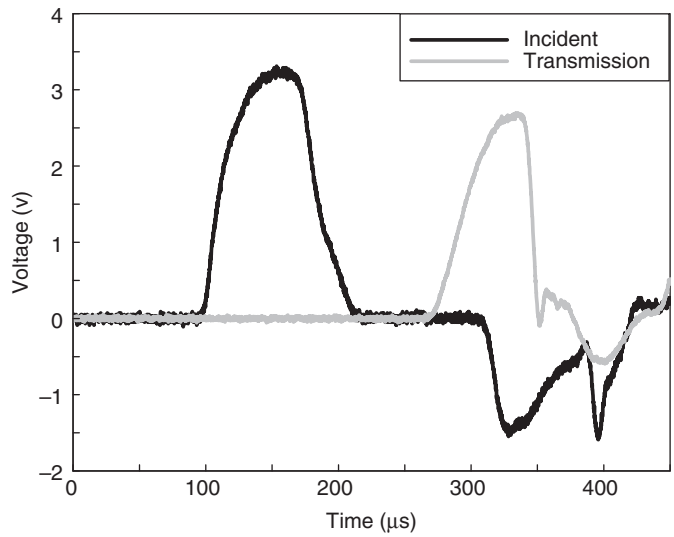

Figure 5. *Typical incident and transmission signals obtained from SHPB tests.*

specimen and the transmission bar, can be extracted from the recorded signals. Figure 6 shows contact forces P_1 and P_2 for the 5° specimen with 20 wt% silica content in the SHPB test. It can be seen that the P_1 and P_2 curves are nearly the same as well as their peak values, and thus, the average of the peak values was taken as the dynamic failure stress of the specimen. It is noted that the strain rate ranges in the dynamic tests are around 400–600 s^{-1}.

RESULTS AND DISCUSSIONS

Failure Mechanism

In an attempt to understand the failure mechanisms, all failed specimens were examined using a microscope. For the 0° specimens, it was found that the failure was mostly dominated by the fiber microbuckling; although, in few cases, the fiber splitting might take place at the specimen ends. However, even though these two failure mechanisms are distinct, no significant differences in the failure stresses were observed. For the 5°, 10°,

Downloaded from jcm.sagepub.com at NATIONAL CHIAO TUNG UNIV LIB on April 24, 2014

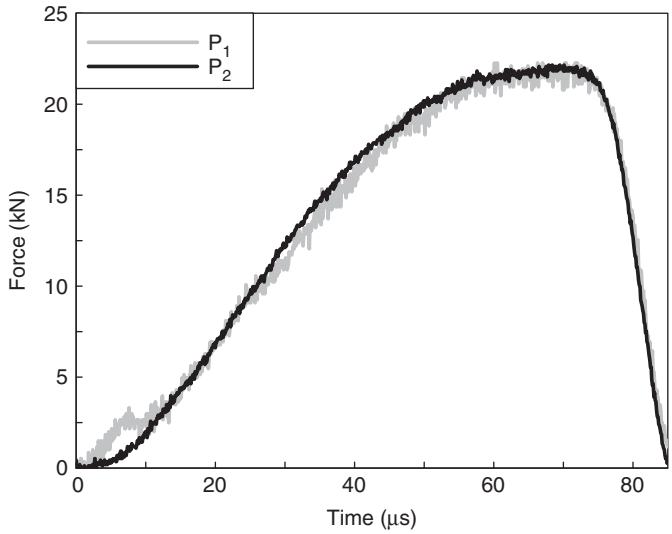

Figure 6. *Time histories of the contact forces for 5° off-axis specimen.*

and 15° specimens, the main failure mechanisms were also the fiber microbuckling. The similar failure mechanism was also reported in the literature [9]. Figures 7 and 8 illustrate the fiber microbuckling of the 0° and 5° samples, respectively. The shining band strips as shown on the photos designate the areas where substantial fiber microbuckling takes place. On the other hand, for 90° samples, the major failure mechanism was the out-of-plane shear failure as shown in Figure 9. It can be seen that the crack in shear mode occurred on the plane orientated around 36°–40° with respect to the loading direction propagating transverse to the fiber direction. Similar failure behaviors were also observed in other polymeric composites systems [13]. Based on the experimental investigations, it was found that the compressive failure mechanism basically was not altered by the contents of silica nanoparticles and the loading rates. In contrast, the compressive failure stresses could be influenced by the silica nanoparticles as well as the loading rates.

Compressive Strength

The experimental data for the off-axis specimens obtained from the quasi-static and dynamic compression tests associated with different fiber orientations are enumerated in Tables 1–5, respectively. It is noted that for each case, at lease four samples were tested. Apparently, the compressive strengths of fiber composites are sensitive to the loading rates, and when the loading rates increase, the materials demonstrate higher failure stresses. Moreover, the compressive strengths of the fiber composites are improved as the silica loading increases, and the incremental percentages caused by the silica nanoparticles in both quasi-static and dynamic cases are almost the same. It is noted that the compressive strength does not seem to increase consistently as particle loading increases. This is especially obvious for the case with silica loading of 20 wt%. The possible reason for the little reduction in the 20 wt% samples could be the larger fiber misalignment generated during the fabrication of the fiber composites. The fiber misalignment, which is a manufacturing

Downloaded from jcm.sagepub.com at NATIONAL CHIAO TUNG UNIV LIB on April 24, 2014

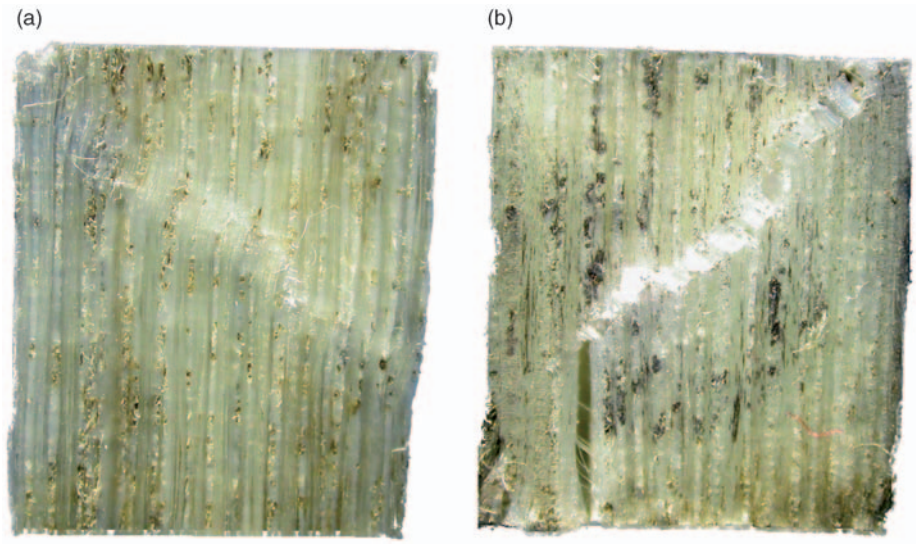

Figure 7. *Microbuckling failure mechanism for 0° specimens: (a) pure epoxy resin, (b) 30 wt% silica nanoparticles.*

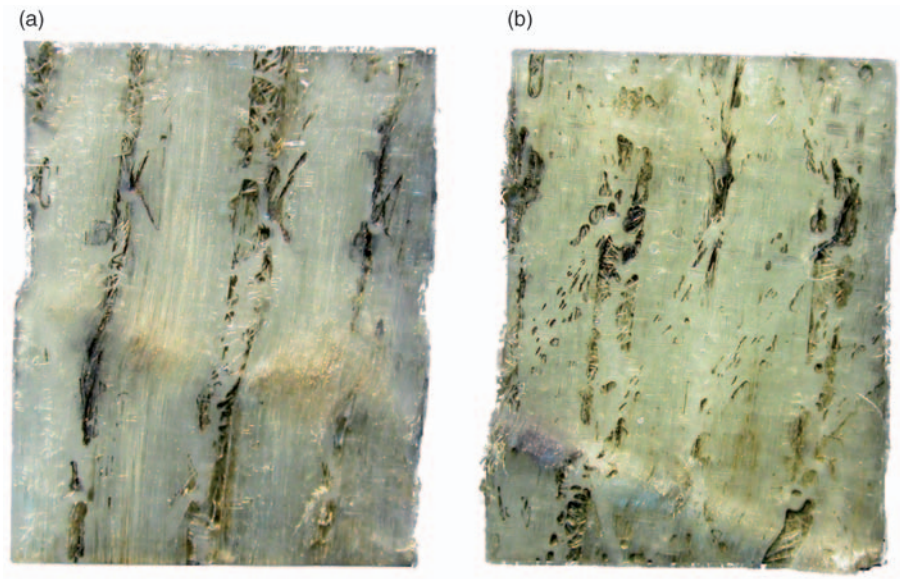

Figure 8. *Microbuckling failure mechanism for 5° specimens: (a) pure epoxy resin, (b) 30 wt% silica nanoparticles.*

defect created by fiber movement in the matrix during the lay-up and curing process may influence the compressive strength of the fiber composites [2,14]. In general, the variation of the fiber misalignment is more significant in the hand-made fiber composites, and this could be responsible for the reduction of the compressive strength in the 20 wt% samples.

Downloaded from jcm.sagepub.com at NATIONAL CHIAO TUNG UNIV LIB on April 24, 2014

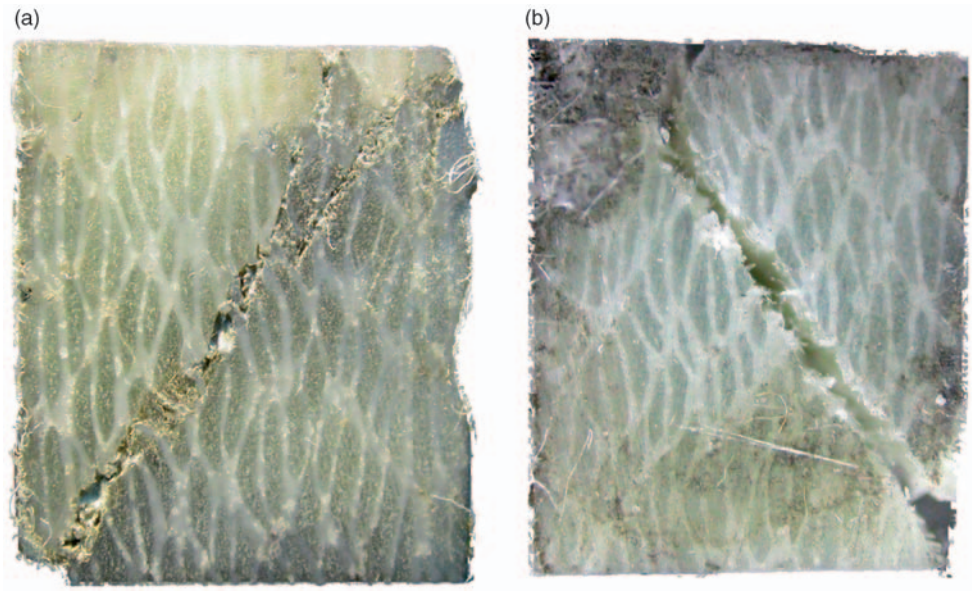

Figure 9. *Out-of-plane shear failure mechanism for 90° specimens: (a) pure epoxy resin, (b) 30 wt% silica nanoparticles.*

For the 0°, 5°, 10°, and 15° samples, the main failure mechanisms are the fiber microbuckling, so the enhancement in compressive strength modified by the silica nanoparticles can be explained using the microbuckling model [2]. In the microbuckling model, the compressive failure was assumed triggered because of fiber microbuckling imbedded in the matrix as shown in Figure 10. By taking into account the nonlinear behavior of the matrix in the bifurcation buckling analysis, Sun and Jun derived the compressive strength of unidirectional fiber composites as the following:

$$\sigma_{11c} = \frac{G_m^{ep}}{1 - c_f}, \tag{1}$$

where G_m^{ep} is the elastic–plastic tangent shear modulus of the matrix, and c_f denotes the fiber volume fraction of the composites. According to Equation (1), it is implied that the compressive strength of the composites can be enhanced if the tangent shear modulus of the matrix is improved. From our previous experiments on the constitutive behaviors of silica/epoxy nanocomposites [15], it was revealed that the Young's modulus of the epoxy matrix was effectively modified by using silica nanoparticles as shown in Figure 11. The improvement occurred not only in the elastic part but also in the nonlinear ranges. Thus, the corresponding tangent modulus of the matrix could be efficiently modified by the nanoparticles and so was the tangent shear modulus if the isotropic property was assumed in the silica/epoxy matrix system. In view of the forgoing, it is quite sensible that the compressive strengths of fiber composites can be appropriately enhanced by silica nanoparticles. In addition, it was depicted that the constitutive behavior of the epoxy matrix is influenced by the loading rate, and when the loading rates are increased, the epoxy materials would become stiffer [16]. Therefore, because of the stiffened behavior of

Downloaded from jcm.sagepub.com at NATIONAL CHIAO TUNG UNIV LIB on April 24, 2014

Table 1. Compressive strengths of 0° specimens with different silica contents.

Silica content (wt%)	Quasi-static compressive strength (MPa)	Increment ratio (%)	Dynamic compressive strength (MPa)	Increment ratio (%)
0	415 ± 18	–	678 ± 7	–
10	452 ± 13	9	706 ± 14	4
20	445 ± 20	7	703 ± 6	4
30	460 ± 16	11	720 ± 22	6

Table 2. Compressive strengths of 5° specimens with different silica contents.

Silica content (wt%)	Quasi-static compressive strength (MPa)	Increment ratio (%)	Dynamic compressive strength (MPa)	Increment ratio (%)
0	227 ± 5	–	531 ± 7	–
10	253 ± 8	11	569 ± 17	7
20	265 ± 8	17	586 ± 4	10
30	275 ± 22	21	618 ± 26	16

Table 3. Compressive strengths of 10° specimen with different silica contents.

Silica content (wt%)	Quasi-static compressive strength (MPa)	Increment ratio (%)	Dynamic compressive strength (MPa)	Increment ratio (%)
0	154 ± 3	–	363 ± 2	–
10	166 ± 10	8	400 ± 20	10
20	163 ± 7	6	387 ± 6	5
30	179 ± 7	16	408 ± 5	12

Table 4. Compressive strengths of 15° specimens with different silica contents.

Silica content (wt%)	Quasi-static compressive strength (MPa)	Increment ratio (%)	Dynamic compressive strength (MPa)	Increment ratio (%)
0	117 ± 3	–	226 ± 4	–
10	123 ± 2	5	252 ± 12	12
20	124 ± 1	6	242 ± 4	7
30	138 ± 6	18	261 ± 20	15

matrix under dynamic loading, the dynamic compressive strengths of the fiber composites are higher than the quasi-static ones. It should be noted that the microbuckling stress given in Equation (1) is evaluated in the fiber direction (0°), and hence, the compressive failure stresses as well as their sensitivity to the silica nanoparticles are dependent on the fiber orientation with respect to the loading direction.

Downloaded from jcm.sagepub.com at NATIONAL CHIAO TUNG UNIV LIB on April 24, 2014

Table 5. Compressive strengths of 90° specimens with different silica contents.

Silica content (wt%)	Quasi-static compressive strength (MPa)	Increment ratio (%)	Dynamic compressive strength (MPa)	Increment ratio (%)
0	46 ± 1	–	77 ± 2	–
10	52 ± 1	13	96 ± 7	25
20	47 ± 1	2	86 ± 3	12
30	60 ± 2	30	112 ± 5	45

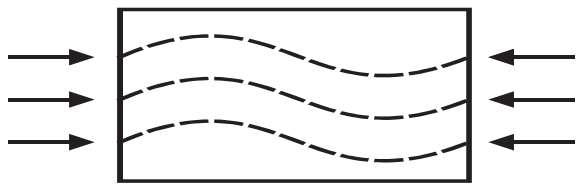

Figure 10. *Microbuckling model.*

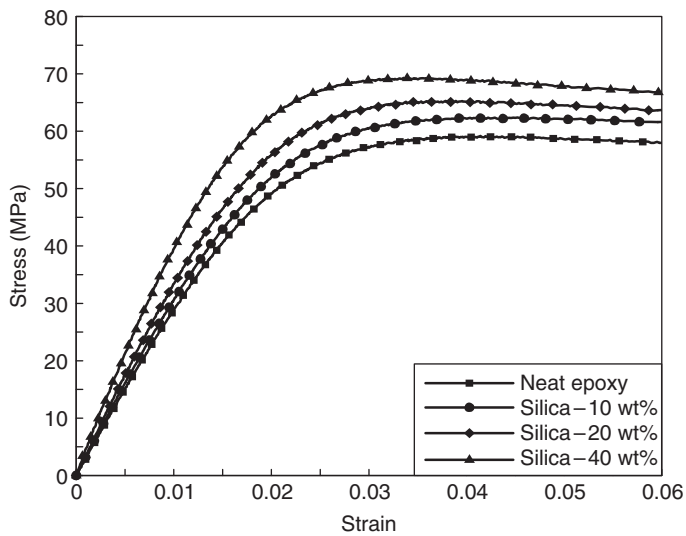

Figure 11. *Stress and strain curves of silica/epoxy nanocomposites with different silica loading.*

On the other hand, for the 90° samples, although the failure mechanism is out of plane shear failure, the failure stresses are also improved by the silica nanoparticles. In order to further understand the enhancing mechanism caused by the silica nanoparticles, the failure surfaces of the samples were examined by the SEM. The SEM micrographs on the fracture surfaces of the samples with pure epoxy resin and 30 wt% silica nanoparticles are compared in Figure 12. It is indicated that for the fiber composites with pure epoxy, the fiber surfaces are quite smooth and featureless without any matrix adhered. It is apparent that the interfacial debonding is the main failure mechanism of the samples. On the contrary,

Downloaded from jcm.sagepub.com at NATIONAL CHIAO TUNG UNIV LIB on April 24, 2014

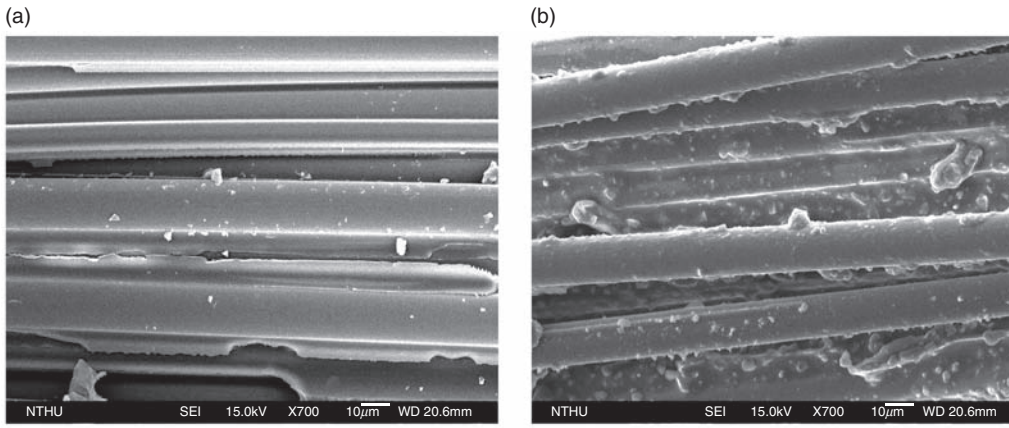

Figure 12. *SEM photos on the failure surfaces of 90° samples: (a) pure epoxy resin, (b) 30 wt% silica particles.*

for the fiber composites with a silica/epoxy matrix, the fiber surfaces were not clean, but they bonded with a little bit of epoxy matrix. Such epoxy adhesion indicates the interfacial bonding between the fiber and matrix was improved, and the interfacial debonding was effectively retarded. Thus, the corresponding improvement in the compressive strength of 90° samples could be a result of the enhanced interfacial bonding modified by the dispersed silica nanoparticles.

CONCLUSIONS

The compressive strengths of off-axis glass/epoxy nanocomposites with different silica nanoparticle loadings were experimentally investigated. Both quasi-static and dynamic compressive behaviors were determined, respectively, using a hydraulic MTS machine and a Hopkinson pressure bar. From experiments, it was revealed that the compressive strengths of 0°, 5°, 10°, and 15° specimens increase with the increment of nanoparticle loadings, and the increasing behaviors were observed in both dynamic and quasi-static cases. Moreover, the main failure modes of the samples were found to be the fiber microbuckling, and thus based on the fiber microbuckling model, and the enhancement could be due to the increment of the modulus of the epoxy matrix made by the silica nanoparticles. On the other hand, for the 90° samples, the compressive strengths were also improved by the silica nanoparticles. From SEM observations on the failure surfaces, it was indicated that the ascending phenomena could be ascribed to the improved interfacial bonding between fibers and surrounding epoxy caused by the silica nanoparticles.

ACKNOWLEDGMENT

This research was supported by the National Science Council, Taiwan, under the contract no. NSC 96-2628-E-009-009 to National Chiao Tung University.

Downloaded from jcm.sagepub.com at NATIONAL CHIAO TUNG UNIV LIB on April 24, 2014

REFERENCES

1. Rosen, B.W. (1965). Mechanics of Composite Strengthening, In: *Fiber Composites Materials*, pp. 35–75, American Society of Metals, Metals Park, OH.
2. Sun, C.T. and Jun, A.W. (1994). Compressive Strength of Unidirectional Fiber Composites with Matrix Non-linearity, *Composites Science and Technology*, **52**(4): 577–587.
3. Argon, A.S. (1972). *Treatise on Materials Science and Technology*, Vol. 1, pp. 1–79, Academic Press, New York.
4. Budiansky, B. and Fleck, N.A. (1993). Compressive Failure of Fibre Composites, *Journal of the Mechanics and Physics of Solids*, **41**(1): 183–211.
5. Subramaniyan, A.K. and Sun, C.T. (2006). Enhancing Compressive Strength of Unidirectional Polymeric Composites Using Nanoclay, *Composites: Part A*, **31**: 2257–2268.
6. Rosso, P., Ye, L., Friedrich, K. and Sprenger, S. (2006). A Toughened Epoxy Resin by Silica Nanoparticle Reinforcement, *Journal of Applied Polymer Science*, **100**(3): 1849–1855.
7. Johnsen, B.B., Kinloch, A.J., Mohammed, R.D., Taylor, A.C. and Sprenger, S. (2007). Toughening Mechanisms of Nanoparticle-modified Epoxy Polymers, *Polymer*, **48**(2): 530–541.
8. Zheng, Y. and Ning, R. (2005). Study of SiO2 Nanoparticles on the Improved Performance of Epoxy and Fiber Composites, *Journal of Reinforced Plastics and Composites*, **24**(3): 223–233.
9. Uddin, M.F. and Sun, C.T. (2008). Strength of Unidirectional Glass/Epoxy Composite with Silica Nanoparticle-enhanced Matrix, *Composites Science and Technology*, **68**: 1637–1643.
10. Adebahr, T., Roscher, C. and Adam, J. (2001). Reinforcing Nanoparticles in Reactive Resins, *European Coatings Journal*, **4**: 144–149.
11. Ninan, L., Tsai, J. and Sun, C.T. (2001). Use of Split Hopkinson Pressure Bar for Testing Off-axis Composites, *International Journal of Impact Engineering*, **25**(3): 291–313.
12. Graff, K.F. (1975). *Wave Motion in Elastic Solids*, Dover Publications, New York.
13. Bazhenov, S.L. and Kozey, V.V. (1991). Transversal Compression Fracture of Unidirectional Fibre-reinforced Plastics, *Journal of Materials Science*, **26**(10): 2677–2684.
14. Yurgartis, S.W. (1987). Measurement of Small Angle Fiber Misalignments in Continuous Fiber Composites, *Composite Science and Technology*, **30**(4): 279–293.
15. Tsai, J.L., Hsiao, H. and Cheng, Y.L. (2007). Investigating Mechanical Behaviors of Nanoparticle Reinforced Composites, In: *Proceedings of the ASC 22th Technical Conference*, Seattle, September.
16. Chen, W., Lu, F. and Cheng, M. (2002). Tension and Compression Tests of Two Polymers Under Quasi-Static and Dynamic Loading, *Polymer Testing*, **21**: 113–121.

Downloaded from jcm.sagepub.com at NATIONAL CHIAO TUNG UNIV LIB on April 24, 2014